BJP British Journal of Pharmacology

DOI:10.1111/bph.12024
www.brjpharmacol.org

RESEARCH PAPER

(*E*)-2,4-bis(*p*-hydroxyphenyl)-2-butenal has an antiproliferative effect on NSCLC cells induced by p38 MAPK-mediated suppression of NF-κB and up-regulation of TNFRSF10B (DR5)

Pushpa Saranya Kollipara[1], Heon Sang Jeong[2], Sang Bae Han[1] and Jin Tae Hong[1]

[1]*College of Pharmacy and Medical Research Center, Chungbuk National University, Cheongju, Korea, and* [2]*College of Agriculture, Life and Environments Sciences, Chungbuk National University, Cheongju, Korea*

Correspondence
Jin Tae Hong, College of Pharmacy, Chungbuk National University 12, Gaeshin-dong, Heungduk-gu, Cheongju, Chungbuk 361-763, Korea.
E-mail: jinthong@chungbuk.ac.kr

Keywords
lung cancer; p38 MAPK; NF-κB; death receptor 5; apoptosis

Received
18 June 2012
Revised
6 September 2012
Accepted
15 October 2012

BACKGROUND AND PURPOSE

The Maillard Reaction Products (MRPs) are known to be effective in chemoprevention. Here we focused on the anticancer effects of (*E*)-2,4-bis(*p*-hydroxyphenyl)-2-butenal (a MRP) on human non-small-cell lung cancer (NSCLC) cells and its mechanism of action.

EXPERIMENTAL APPROACH

We analysed the activity of (*E*)-2,4-bis(*p*-hydroxyphenyl)-2-butenal on NSCLC cells (NCI-H460 and A549) by use of Western blot analysis for major apoptotic proteins, MAPK, NF-κB and death receptor expression. We also used RT-PCR to determine its effects on death receptor mRNA expression, EMSA for effects on NF-κB DNA binding activity and colony formation assay for effects of inhibitors on (*E*)-2,4-bis(*p*-hydroxyphenyl)-2-butenal's actions.

KEY RESULTS

(*E*)-2,4-bis(*p*-hydroxyphenyl)-2-butenal induced a concentration (10–40 μg·mL^{-1})- and time (30 min–72 h)-dependent inhibitory effect on the growth of NSCLC cells due to induction of apoptosis. Concomitantly, it significantly increased the expression of apoptotic proteins such as cleaved caspase-3, cleaved caspase-9, Bax and p53, but down-regulated the expression of anti-apoptotic proteins Bcl-2, cIAP1 and cIAP2. This effect was induced by up-regulation of MAPK and death receptor proteins TNFRSF12, TNFRSF10B and TNFRSF21, but suppression of NF-κB. Of the death receptors activated, only TNFRSF10B knock down with siRNA reversed the effect of (*E*)-2,4-bis(*p*-hydroxyphenyl)-2-butenal. Even though all the MAPKs were activated, only pretreatment with a p38 MAPK inhibitor reversed (*E*)-2,4-bis(*p*-hydroxyphenyl)-2-butenal-induced cell growth inhibition, increase in cleaved caspase-3, -9 and TNFRSF10B expression, and NF-κB inactivation.

CONCLUSIONS AND IMPLICATIONS

(*E*)-2,4-bis(*p*-hydroxyphenyl)-2-butenal induces apoptosis in NSCLC cells by p38 MAPK-mediated suppression of NF-κB and activation of TNFRSF10B, which then activates the caspase-3 and caspase-9 pathways.

Abbreviations

NSCLC, non small cell lung cancer

Introduction

Lung cancer is the most common cancer in terms of both incidence and mortality and is the second leading cause of cancer-related deaths worldwide (Nesbitt *et al.*, 1997). Although combination chemotherapy constitutes a major part of the treatment programme for patients with inoperable lung cancer, improvements in treatment efficacy, even with newly developed anticancer agents, have been unsatisfactory (Rigas, 1998). Thus, there is a need for novel therapeutics with specific targets for the treatment of lung cancer.

Death receptors are members of the TNF receptor super family and comprise a sub-family that is characterized by an intracellular death domain. Death receptors are activated by their natural ligands, the TNF family. The interaction of the TNF family of ligands with their cognate receptors leads to cell growth, differentiation, survival or death, depending on the cellular context and the nature of the ligand and receptor interaction (Locksley *et al.*, 2001). Of all the death receptors TNF-related apoptosis-inducing ligand TNFRSF10A (TRAIL-R1) and TNFRSF10B (TRAIL-R2) are selectively expressed in cancer cells and thus offer an advantage for targeted therapy and prevention (Srivastava, 2000; 2001; Shankar and Srivastava, 2004). The balance between these positive and negative regulators ultimately determines the fate of a cell (Baud and Karin, 2001; Ashkenazi, 2002; Karin and Lin, 2002). The expression of death receptors induces activation of caspase-8, which leads to the activation of downstream caspases, including caspases-9 and -3, as well as the translocation of Bax to mitochondria leading to apoptosis (Elrod and Sun, 2008).

The signalling event involved in survival, growth arrest, or programmed cell death includes activation of the MAPK pathway (Schwenger *et al.*, 1998). The MAPK pathways consist of p38 MAPK (p38), ERK and JNK. It is primarily activated by stress signals, and its activation leads to inhibition of cellular proliferation and/or decreased cell survival. Metformin treatment of lung cancer cells activates the JNK/p38 MAPK signalling pathway and caspases. Blockade of the JNK/p38 MAPK pathway prevented the apoptosis-inducing effect of metformin (Wu *et al.*, 2011). Moreover, previous reports have indicated that p38 is the upstream target of TNFRSF10B induced by other agents (Lei *et al.*, 2008; Park *et al.*, 2010). In human oral cancer cells, phenethyl isothiocyanate activates TNFRSF10B to induce apoptosis via p38 MAPK (Huong *et al.*, 2012). AW00179 is able to sensitize H1299 human lung cancer cells to TRAIL-mediated apoptosis through two distinct mechanisms: the ROS-JNK-c-Jun-(MAPK) pathway mediated by up-regulation of TNFRSF10B, and down-regulation of antiapoptotic molecules (Hwang *et al.*, 2012b). Taken together, these data show that a specific MAPK pathway could be activated to regulate the death receptor and would depend on the compound being used to induce lung cancer cell death.

Members of the NF-κB family also play an important role in the development and progression of several human malignancies (Nakshatri *et al.*, 1997; Baud and Karin, 2009). NF-κB gene products have also been shown to have important proliferative and anti-apoptotic activities that could contribute to the development, progression and resistance to therapy of tumour cells (Karin and Greten, 2005; Viatour *et al.*, 2005). Thus, the activation of NF-κB is correlated with apoptotic resistant and anti-apoptotic properties. Recent studies on the signalling mechanisms of the DR have revealed that members of the NF-κB and caspase families are key regulators of cell death. Several studies have demonstrated that activation of MAPK, which controls the activation of NF-κB and IKKs, is significantly involved in the regulation of cancer cell growth (Lee *et al.*, 1997; Wang *et al.*, 2000; Kim *et al.*, 2004; Moon *et al.*, 2007). The activated p38 MAPK leads to activation of the TNFRSF10B-induced apoptosis pathways through the modulation of NF-κB activity (Wang *et al.*, 2000; Lei *et al.*, 2008; Park *et al.*, 2010).

Several compounds that have anti-oxidant and anti-inflammatory properties also have anticancer effects (Lee *et al.*, 2011b). Recently, we synthesized (*E*)-2,4-bis(*p*-hydroxyphenyl)-2-butenal by the Maillard reaction (MR) with tyrosine and fructose, using a high temperature and pressure treatment (Hwang *et al.*, 2012a). These Maillard reaction products (MRPs) such as glucose-tyrosine, glucose-lysine, fructose-lysine, ribose-lysine and xylose-tryptophan have antioxidant and anti-mutagenic effects (Jing and Kitts, 2004; Atrooz, 2008). Previously, it was shown that (*E*)-2,4-bis(*p*-hydroxyphenyl)-2-butenal induces antioxidant and anti-inflammatory effects by inhibition of NF-κB and STAT3 activity (Lee *et al.*, 2011a). To investigate the anticancer activity of (*E*)-2,4-bis(*p*-hydroxyphenyl)-2-butenal, we examined its effect on NSCLC cell growth and signalling mechanisms.

Methods

Chemicals

In brief, (*E*)-2,4-bis(*p*-hydroxyphenyl)-2-butenal was prepared as follows. We prepared 100 mL of fructose–tyrosine mixture including 0.1 M tyrosine and 0.05 M fructose. MR was carried out in a temperature-controlled autoclave apparatus (Jisico, Seoul, South Korea) at 130°C for 2 h. Then the reaction mixture was filtered through a 0.45 μm membrane and several fractionation steps were used to isolate the active compounds, as described elsewhere (Hwang *et al.*, 2012a). (*E*)-2,4-bis(*p*-hydroxyphenyl)-2-butenal was dissolved in 0.01% DMSO and used at concentrations of 10, 20, 30, 40 $\mu g \cdot mL^{-1}$ to treat cultured cells.

Cell culture

NCI-H460 and A549 human lung cancer cells were obtained from the American Type Culture Collection (Cryosite, Lane Cove, NSW, Australia). LL-24 normal lung cells were obtained from the Korean cell line bank. NCI-H460, LL-24 and A549 human lung cancer cells were grown in RPMI1640 and DMEM, respectively, with 10% FBS, 100 $U \cdot mL^{-1}$ penicillin and 100 $\mu g \cdot mL^{-1}$ streptomycin, at 37°C in 5% CO_2 humidified air.

Cell viability assay

To determine the cell viability the cells were cultured in 24-well plates at a density of 5×10^4 cells per well. The cells were treated with different concentrations of (*E*)-2,4-bis(*p*-hydroxyphenyl)-2-butenal (10–40 $\mu g \cdot mL^{-1}$). At different time points the cultured cells were trypsinized with TrypLE Express (Invitrogen), and then the cells were pelleted by centrifuga-

tion for 5 min at 151× *g*. Cells were resuspended in PBS, and 0.2% trypan blue was added to the cancer cell suspension. Subsequently, a drop of suspension was placed into a Neubauer chamber, and the living cancer cells were counted. Cells that showed signs of staining were considered to be dead, whereas those that excluded trypan blue were considered viable. Each assay was carried out in triplicate.

Detection of apoptosis

The apoptosis assay was first performed by using DAPI staining. NCI-H460 and A549 human lung cancer cells were cultured in the absence or presence of increasing concentrations of (*E*)-2,4-bis(*p*-hydroxyphenyl)-2-butenal, and induction of apoptotic cell death was evaluated after 24 h. Apoptotic cells were determined by observing the morphological changes after DAPI staining under a fluorescence microscope (DAS microscope, 100× or 200×: Leica Microsystems, Inc., Deefield, IL). Apoptosis was also evaluated by the TUNEL staining assay. In brief, cells were cultured on eight-chamber slides. After treatment with (*E*)-2,4-bis(*p*-hydroxyphenyl)-2-butenal (10–40 μg·mL^{-1}) for 24 h, the cells were washed twice with PBS and fixed by incubation in 4% paraformaldehyde in PBS for 1 h at room temperature. The TUNEL assays were performed by using an *in situ* Cell Death Detection Kit (Roche Diagnostics GmbH, Mannheim, Germany), according to the manufacturer's instructions. The total number of cells in a given area was determined by using DAPI and TUNEL staining. The apoptotic index was determined as the number of DAPI-stained TUNEL-positive cells divided by the total number of cells counted ×100.

Western blot analysis

Harvested cells were homogenized with lysis buffer [50 mM Tris pH 8.0, 150 mM NaCl, 0.02% sodium azide, 0.2% SDS, 1 mM PMFS, 10 μl·mL^{-1} aprotinin, 1% igapel 630 (Sigma Aldrich, St. Louis, MO), 10 mM NaF, 0.5 mM EDTA, 0.1 mM EGTA and 0.5% sodium deoxycholate] and centrifuged at 23 000× *g* for 15 min. The protein concentration was measured by the Bradford method (Bio-Rad Protein Assay; Bio-Rad Laboratories Inc., Hercules, CA), and equal amounts of proteins (50 μg) were separated on a SDS/10%-polyacrylamide gel and then transferred to a Hybond ECL nitrocellulose membrane (Amersham Pharmacia Biotech Inc., Piscataway, NJ). Blots were blocked for 2 h at room temperature with 5% (w v^{-1}) non-fat dried milk in Tris-buffered saline [10 mM Tris (pH 8.0) and 150 mM NaCl] solution containing 0.05% Tween-20. The membrane was incubated for 5 h at room temperature with specific antibodies: mouse polyclonal antibodies against Bax, p53, IκB, p- IκB, p65, histone-H1, p-ERK, p-p38, TNFRSF1A, TNFRSF10A, TNFRSF10B, MMP-9 cyclin D and Fas (1:500 dilution; Santa Cruz Biotechnology Inc., Santa Cruz, CA); rabbit polyclonal for p50, p38, ERK, JNK, TNFRSF1B, TNFRSF12 and TNFRSF21 (1:500 dilution, Santa Cruz Biotechnology Inc.); and for caspase-3, cleaved caspase3, cleaved caspase-9, inhibitor of apoptosis protein (cIAP) 1 and 2, p-JNK, COX-2 and VEGF (1:1000 dilution; Cell Signaling Technology, Inc., Beverly, MA). The blot was then incubated with the corresponding conjugated anti-rabbit and anti-mouse immunoglobulin G-HRP (1:4000 dilution; Santa Cruz Biotechnology Inc.). Immunoreactive proteins were detected with the ECL Western blotting detection system. The relative density of the protein bands was scanned by densitometry using MyImage (SLB) and quantified by Labworks 4.0 software (UVP Inc.).

Gel EMSA

The gel shift assay was performed according to the manufacturer's recommendations (Promega, Madison, WI). Briefly, the sample of 1 × 10^6 cells·mL^{-1} was washed twice with 1 × PBS, followed by the addition of 1 mL of PBS, and the cells were scraped into a cold Eppendorf tube. Cells were pelleted by centrifugation at 151× *g* for 5 min, and the resulting supernatant was removed. Solution A (50 mM HEPES, pH 7.4, 10 mM KCl, 1 mM EDTA, 1 mM EGTA, 1 mM dithiothreitol, 0.1 μg·mL^{-1} PMSF, 1 μg·mL^{-1} pepstatin A, 1 μg·mL^{-1} leupeptin, 10 μg·mL^{-1} soybean trypsin inhibitor, 10 μg·mL^{-1} aprotinin and 0.5% Nonidet P-40) was added to the pellet and allowed to incubate on ice for 10 min and centrifuged at 3,220× *g* for 6 min and cytoplasmic extract was separated. Solution C (solution A + 10% glycerol and 400 mM KCl) was added to the pellet and vortexed on ice for 20 min. The cells were centrifuged at 13,000× *g* for 12 min, and the resulting nuclear extract supernatant was collected in a chilled Eppendorf tube. Consensus oligonucleotides were end-labelled using T4 polynucleotide kinase and [γ-^{32}P]-ATP for 10 min at 37°C. Gel shift reactions were assembled and allowed to incubate at room temperature for 10 min followed by the addition of 1 μL (50 000–200,000 cpm) of labelled oligonucleotide and another 20 min of incubation at room temperature. Subsequently, 1 μL of gel loading buffer was added to each reaction and loaded onto a 4% non-denaturing gel and electrophoresis was performed until the dye was three-quarters of the way down the gel. The gel was dried at 80°C for 50 min and exposed to film overnight at −70°C. The relative density of the DNA-protein binding bands was scanned by densitometry using My Image (SLB, Seoul, Korea) and quantified by Lab works 4.0 software (UVP Inc., Upland, CA).

RT-PCR

Total RNAs were isolated from cultured cells using RNeasy plus Mini Kit (Qiagen, Seoul, South Korea) according to the manufacturer's manual. The RNA pellet obtained in the final step was dissolved in 30 μL of sterile diethylpyrocarbonate (DEPC)-treated water, and its concentration was determined using a UV spectrophotometer at 260 nm. RNA was kept in DEPC-treated water at −70°C until use. Reverse transcription was performed using a High Capacity RNA-to-cDNA Kit (AB). PCR amplifications were then carried out with the primers. The PCR primers used were 5′-ACCAATGCCACAAAGGAAC-3′ and 5′-CTGCAATTGAAGCACTGGAA-3′ for the human TNFRSF1A, 5′-CTCAGGAGCATG GGGATAAA-3′ and 5′-AGC CAGCCAGTCTGACATCT-3′ for the human TNFRSF1B, 5′-ATGGCGATGGCTGCGTGTCCTG-3′ and 5′-AGCGCCTCC TGGGTCTCGGGGTAG-3′ for the human TNFRSF12, 5′-ACTTTGGTTGTTCCGTTGCTGTTG-3′ and 5′-GGCTTTC CATTTGCTGCTCA-3′ for the human TNFRSF10A, 5′-TGGAACAACGGGGACAGAACG-3′ and 5′-GCAGCGCAAGC AGAAAAGGAG-3′ for the human TNFRSF10B, 5′-AAGCCGG GGACCAAGGAGACAGACAAC-3′ and 5′-TGCCGGGGCC CTTTTTCAGAGT-3′ for the human TNFRSF21 and 5′-CAA

AGCCCATTTTTCTTCCA-3′ and 5′-GACAAAGCCACCCCA AGTTA-3′ for human FAS, 5′-CAGCTCTTCCACCTA CAGAAGG-3′ and 5′-AAGATTGAACACTGCCCCCAGG-3′ for FasL, 5′-AGACCTGCGTGCTGATCGTG-3′ and 5′-TTATTTT GCGGCCCAGAGCC-3′ for human TRAIL, 5′-GAAGGTGAAG GTCGGAGT-3′ and 5′-CTTCTACCACTACCCTAAAG-3′ for GAPDH respectively.

Clonogenic assay

This assay tests every cell in a given population for its ability to undergo unlimited division and form colonies. In brief, NCI-H460 and A549 cell were pretreated with a p38 MAPK inhibitor. After 30 min, 8×10^3 cells·mL^{-1} were suspended in 2 mL of 0.3% agar containing basal medium Eagle's agar containing 10% FBS. The cultures were maintained at 37°C in a 5% CO_2 atmosphere for 2 weeks, and cell colonies >80 μm in diameter were scored.

Confocal microscopy

NCI-H460 and A549 cells were plated in the chamber slides at a density of 5×10^3 cells per chamber. The cells were then treated with (*E*)-2,4-bis(*p*-hydroxyphenyl)-2-butenal or media. One hour later, the cells were washed once with PBS and fixed with 4% paraformaldehyde for 20 min, membrane-permeabilized by exposure to 0.1% Triton X-100 for 2 min in PBS and placed in blocking serum (5% BSA in PBS) at room temperature for 2 h. The cells were then exposed to primary rabbit and mouse polyclonal antibody for p50 and p65, respectively (1:50 dilution; Santa Cruz Biotechnology Inc., Santa Cruz, CA), overnight at 4°C. After being washed with ice-cold PBS, followed by treatment with an anti-rabbit secondary antibody labelled with Alexa Fluor 568 and 488(1:100 dilution, Molecular Probes Inc., Eugene, OR) for 2 h at room temperature, immunofluorescence images were acquired using a confocal laser scanning microscope (TCS SP2, Leica Microsystems AG, Wetzlar, Germany) equipped with a 630× oil immersion objective.

Results

(E)-2,4-bis(p-hydroxyphenyl)-2-butenal inhibited NCI-H460 and A549 human lung cancer cell growth

Initially, to examine the effect of (*E*)-2,4-bis(*p*-hydroxyphenyl)-2-butenal on NCI-H460 and A549 human lung cancer cell growth, we analysed the growth pattern of the cells with different concentrations of (*E*)-2,4-bis(*p*-hydroxyphenyl)-2-butenal at various time points. Morphological features of the NCI-H460 and A549 cells show a reduction in cell size and rounding up of cells in a time-dependent (24–72 h) and concentration-dependent manner (10–40 μg·mL^{-1}). The cell growth inhibition effect of (*E*)-2,4-bis(*p*-hydroxyphenyl)-2-butenal was also evaluated by the trypan blue dye exclusion method. (*E*)-2,4-bis(*p*-hydroxyphenyl)-2-butenal decreased the cell numbers in a concentration- and time-dependent manner (Figure 1A). The IC_{50} values at 48 h were 30.4 and 31.0 μg·mL^{-1} in NCI-H460 and A549 cells respectively. (*E*)-2,4-bis(*p*-hydroxyphenyl)-2-butenal had no effect on normal lung cells LL-24.

(E)-2,4-bis(p-hydroxyphenyl)-2-butenal induced apoptotic cell death

To find out whether the inhibition of cell growth by (*E*)-2,4-bis(*p*-hydroxyphenyl)-2-butenal was due to the induction of apoptotic cell death; we evaluated changes in the chromatin morphology of cells using DAPI staining. To further characterize the apoptotic cell death induced by (*E*)-2,4-bis(*p*-hydroxyphenyl)-2-butenal, we performed TUNEL staining assays, and then the labelled cells were analysed by fluorescence microscopy. Cells were labelled by the TUNEL assay and both NCI-H460 and A549 human lung cancer cells showed increased fluorescence intensity in the presence of (*E*)-2,4-bis(*p*-hydroxyphenyl)-2-butenal (Figure 1B). The number of apoptotic cells (DAPI-positive TUNEL-stained cells) in NCI-H460 and A549 human lung cell cultures was increased in the presence of increasing concentrations of (*E*)-2,4-bis(*p*-hydroxyphenyl)-2-butenal, to about 86% and 83% of cells, respectively, at a concentration of 40 μg·mL^{-1}.

Effect of (E)-2,4-bis(p-hydroxyphenyl)-2-butenal on the expression of apoptotic regulatory proteins

To confirm the effects of (*E*)-2,4-bis(*p*-hydroxyphenyl)-2-butenal on apoptotic cell death, we also analysed the expression levels of various apoptotic signalling proteins. (*E*)-2,4-bis(*p*-hydroxyphenyl)-2-butenal increased the levels of apoptotic regulatory proteins, such as cleaved caspase-9, BAX and p53, in both the cell lines in a time-dependent manner (Figure 2A). At the same time, we also analysed the expression of various pro-apoptotic and antiapoptotic proteins in the presence of various concentrations (10–40 μg·mL^{-1}) of (*E*)-2,4-bis(*p*-hydroxyphenyl)-2-butenal. Again, we observed that as the concentration of (*E*)-2,4-bis(*p*-hydroxyphenyl)-2-butenal was increased, the expression of apoptosis-inducing proteins, cleaved caspase-3, cleaved caspase-9, BAX and p53, was also increased. Similarly as the concentration increased, the expression of the anti-apoptotic proteins (Bcl-2, cIAP1 and cIAP2) was decreased (Figure 2B).

Regulation of death receptors activity by (E)-2,4-bis(p-hydroxyphenyl)-2-butenal

Death receptors can be the target of many apoptotic stimulators. Hence, we performed RT-PCR to find the expression levels of various receptors including TNF receptors (TNFRSF1A and TNFRSF1B) and death receptors (TNFRSF12, TNFRSF10B and TNFRSF21). The results showed a decrease in the expression of the TNF receptors. However, there was an increase in the expression of TNFRSF12, TNFRSF10B and TNFRSF21 in both NSCLC cell lines treated with 30 μg·mL^{-1} of (*E*)-2,4-bis(*p*-hydroxyphenyl)-2-butenal when compared with the untreated control. In addition to RT-PCR, Western blot analysis also showed an increase in death receptor expression (Figure 2C and D). These findings indicate that (*E*)-2,4-bis(*p*-hydroxyphenyl)-2-butenal interacts with receptors to induce apoptosis in NCI-H460 and A549 NSCLC cell lines.

Inhibition of NF-κB activation by (E)-2,4-bis(p-hydroxyphenyl)-2-butenal

A decreased in activity of NF-κB has been shown to be involved in apoptotic cell death in many cancer cells. Hence,

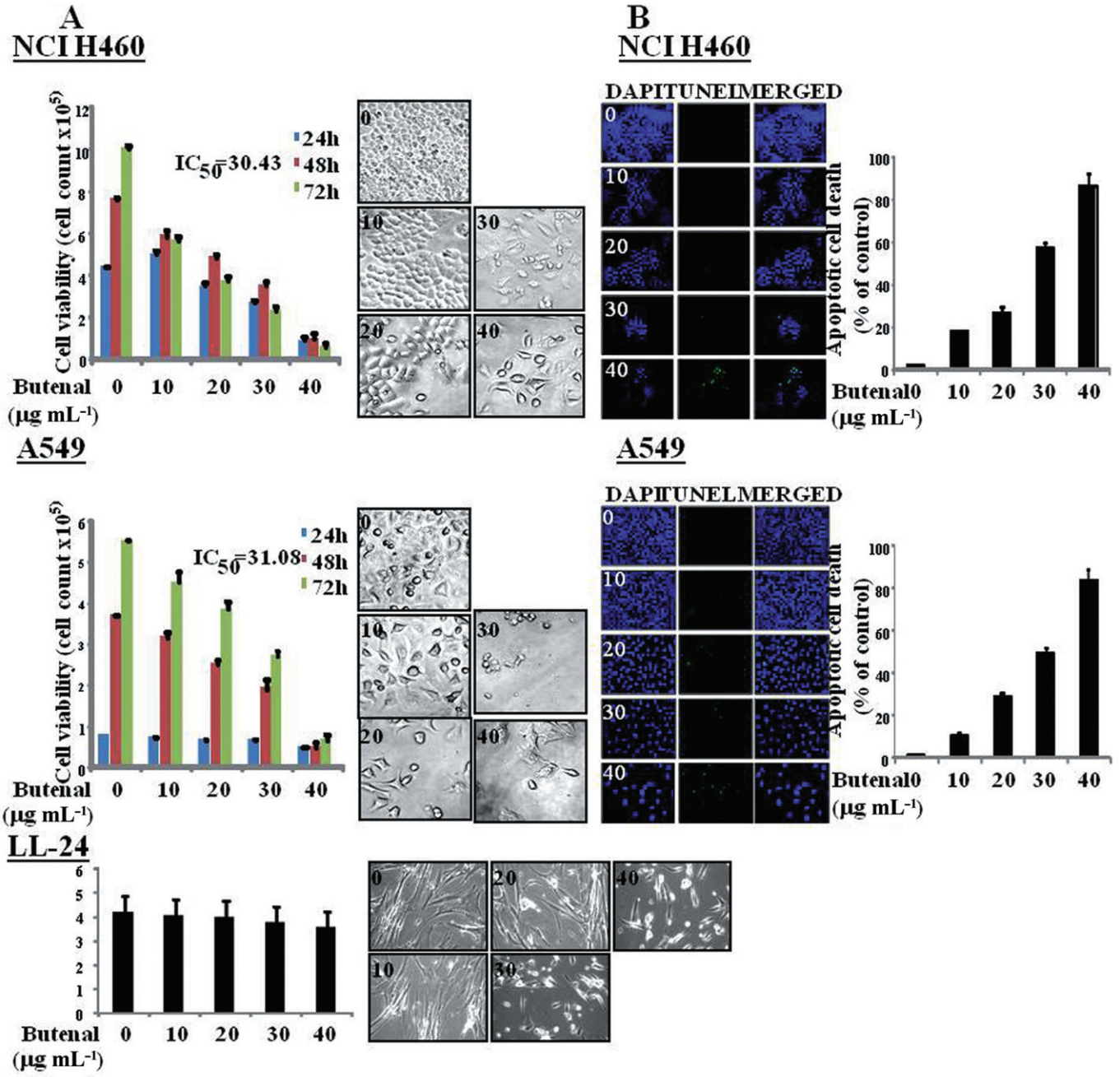

Figure 1

Effect of (*E*)-2,4-bis(*p*-hydroxyphenyl)-2-butenal on the cell viability and morphological changes of NSCLC cell lines. (A) Concentration- and time-dependent effect of (*E*)-2,4-bis(*p*-hydroxyphenyl)-2-butenal on cell viability of NCI-H460, A549 and LL-24 cells. After treatment with (*E*)-2,4-bis(*p*-hydroxyphenyl)-2-butenal (0–40 μg·mL^{-1}) for 24, 48 and 72 h, the morphological changes of NCI-H460 and A549 were observed and the number of viable cells was counted under a microscope (magnification, ×200). Values are mean ± SD of three experiments with replicates. **P* ≤ 0.05 indicates statistically significant differences from the control group. (B) Apoptotic cell death of NSCLC cell lines with the treatment of (*E*)-2,4-bis(*p*-hydroxyphenyl)-2-butenal. Quantification of apoptosis by TUNEL assay. The green colour in the fixed cells marks TUNEL-labelled cells. Total number of cells in a given area was determined by using DAPI nuclear staining (fluorescent microscope). The apoptotic index was determined as the DAPI-stained TUNEL-positive cell number/total DAPI-stained cell number (magnification, ×200). Values are mean and SD of three experiments with replicates. **P* ≤ 0.05 indicates statistically significant differences from the control group.

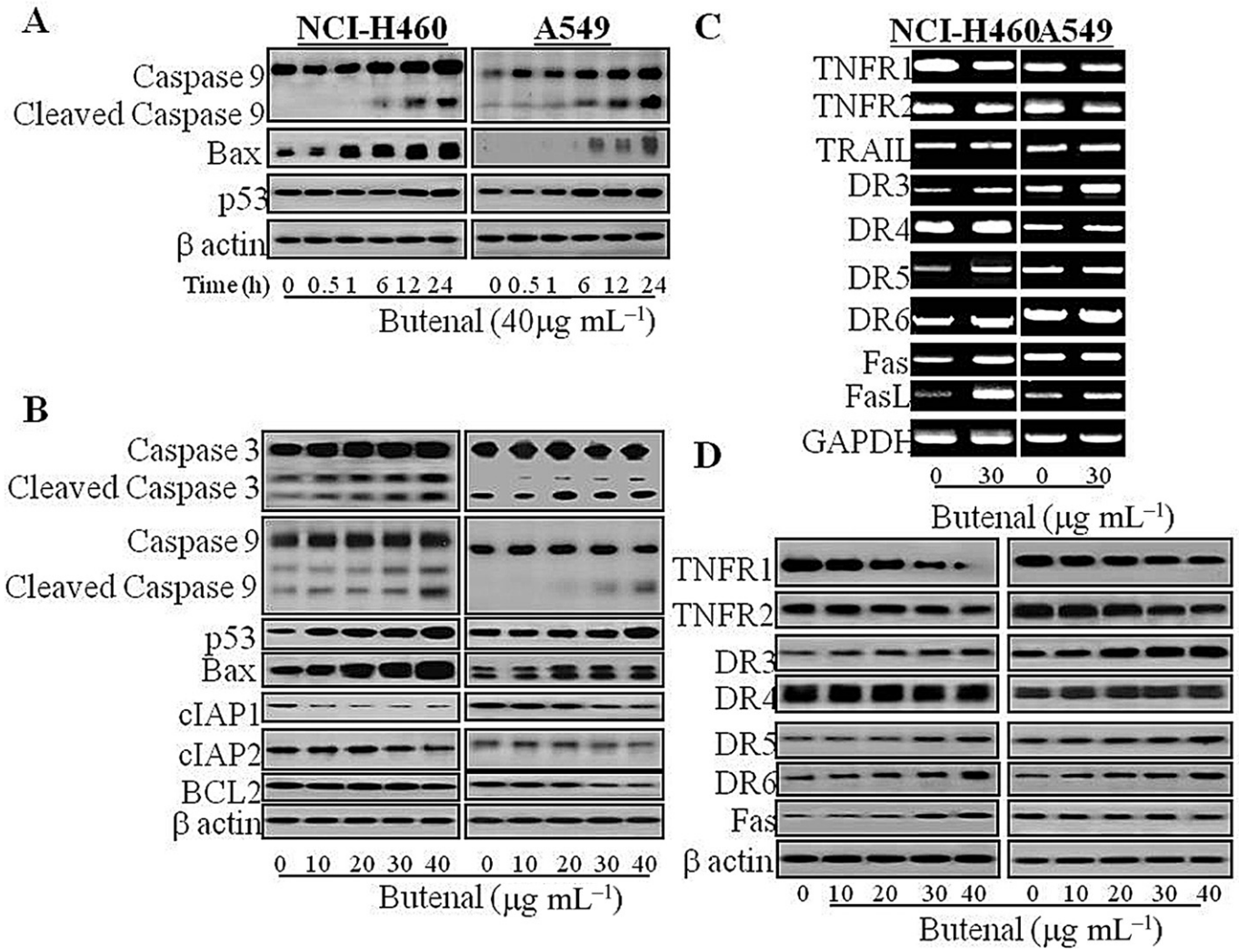

Figure 2

Effect of (*E*)-2,4-bis(*p*-hydroxyphenyl)-2-butenal on the expression of apoptosis regulatory proteins. (A) The cells were treated with same concentration (40 μg·mL^{-1}) of (*E*)-2,4-bis(*p*-hydroxyphenyl)-2-butenal and harvested at different time points. (B) The cells were treated with different concentrations (0–40 μg·mL^{-1}) of (*E*)-2,4-bis(*p*-hydroxyphenyl)-2-butenal at 37°C for 12 h. Equal amounts of total proteins (50 μg per lane) were subjected to 10% SDS-PAGE. Expressions of cleaved caspase-3, cleaved caspase-9, p53, Bax, cIAP1/2, Bcl-2 and β-actin were detected by Western blotting using specific antibodies. β-Actin protein was used an internal control in NCI-H460 and A549 lung cancer cells. Each band is representative of three independent experiments. (C) Effect of (*E*)-2,4-bis(*p*-hydroxyphenyl)-2-butenal on death receptor expression in NSCLC cell lines. The cells were treated with different concentrations (0–40 μg·mL^{-1}) of (*E*)-2,4-bis(*p*-hydroxyphenyl)-2-butenal at 37°C, and total RNA were extracted and examined for expressions of TNFRSF1A and 1B, TNF-R1 and 2, FAS, TNFRSF12, 10A, 10B and 21 (DR-3, -4, -5, -6) and GAPDH by RT-PCR. GAPDH was used as an internal control to show equal RNA loading. Equal amounts of total proteins (50 μg·per lane) were subjected to 10% SDS-PAGE. Expressions of TNFRSFs, FAS, and β-actin were detected by Western blotting using specific antibodies. β-Actin protein was used an internal control. Each band is representative for three experiments.

we examined the DNA binding activity of NF-κB with EMSA. (*E*)-2,4-bis(*p*-hydroxyphenyl)-2-butenal induced a concentration-dependent decrease in the DNA binding activity of NF-κB (Figure 3A). To interpret the EMSA results, we performed Western blotting for the NF-κB proteins. Along with the inhibitory effect on NF-κB DNA binding activity, we also found that (*E*)-2,4-bis(*p*-hydroxyphenyl)-2-butenal concentration-dependently inhibited the translocation of p50 and p65 into the nucleus by inhibiting the phosphorylation of IκB (Figure 3B). Furthermore, to assess the intracellular location of p50 and p65 subunits, we performed confocal microscopy and found that there was a significant inhibition of translocation of p50 and p65 into the nucleus. This was depicted as a decrease in the intensity of staining in the nucleus and increase in the cytosol of the (*E*)-2,4-bis(*p*-hydroxyphenyl)-2-butenal-treated cells (Figure 3C).

Activation of the MAPK pathway by (E)-2,4-bis(p-hydroxyphenyl)-2-butenal

The MAPK protein is essential for the induction of apoptosis in various cancer cells. Thus, we investigated the changes in the expression of MAPK proteins (ERK, JNK and p38) induced

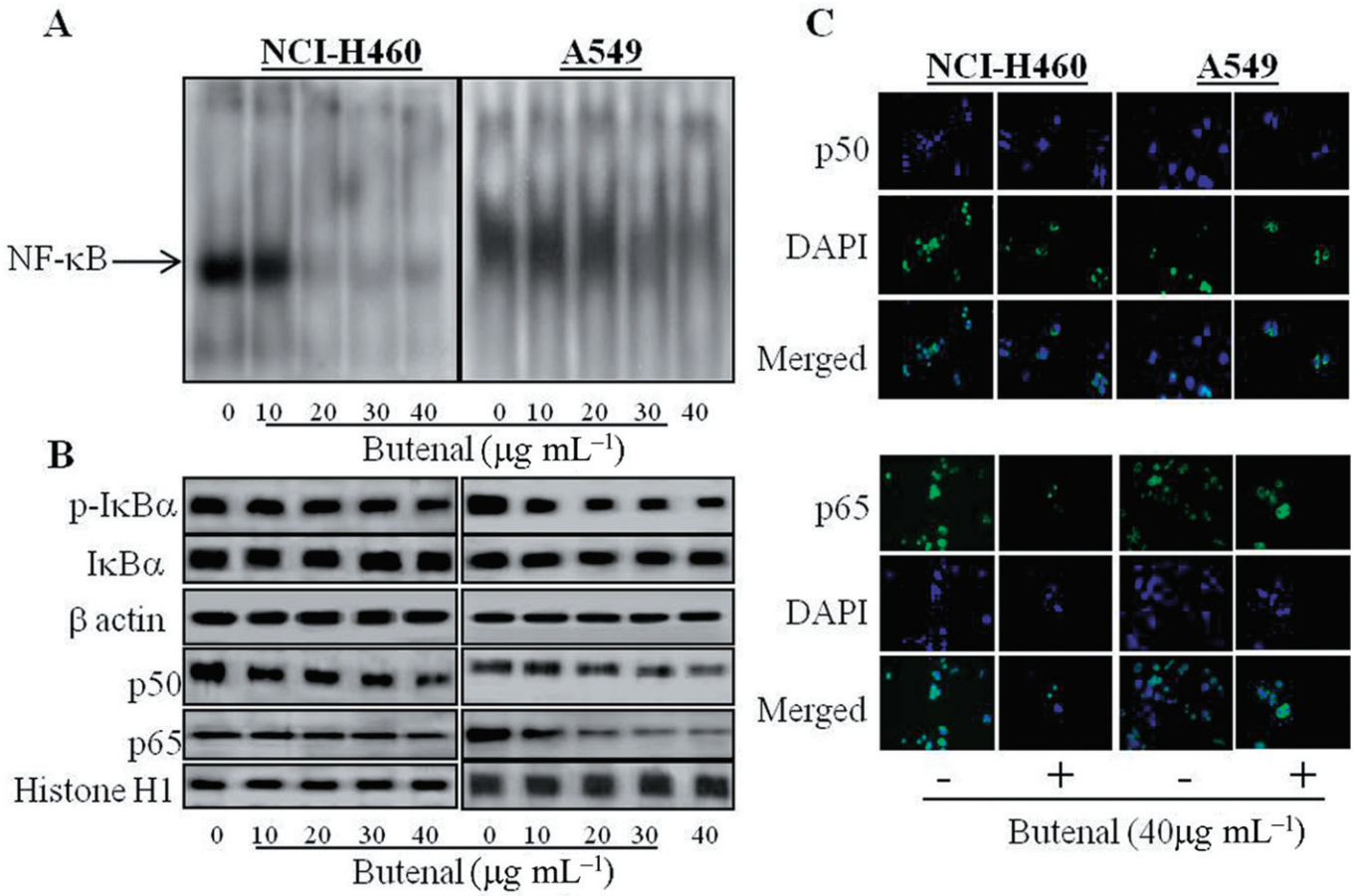

Figure 3

Effect of (*E*)-2,4-bis(*p*-hydroxyphenyl)-2-butenal on NF-κB activation in NSCLC cell lines. (A) Nuclear extracts from NCI-H460 and A549 lung cancer cells treated with (*E*)-2,4-bis(*p*-hydroxyphenyl)-2-butenal (0–40 μg·mL^{-1}) for 1 h were incubated in binding reactions of ^{32}P-end-labelled oligonucleotide containing the κB sequence. The activation of NF-κB was investigated using EMSA as described in Methods. (B) The cells treated with (*E*)-2,4-bis(*p*-hydroxyphenyl)-2-butenal (0–40 μg·mL^{-1}) for 1 h were lysed, cytosolic proteins were used to determine the expression of IκB, p-IκB and β-actin (internal control) and nuclear proteins were used to determine the expression of p50, p65 and histoneH1(internal control) in lung cancer cells. (C) Intracellular location of p50 and p65 in lung cancer cells was determined by immunofluorescence confocal scanning microscope (magnification, 400×). Double staining (Merge) with p50 or p65 and DAPI staining demonstrates the localization of p50 and p65 in the nucleus. Values are mean ± SD of three experiments with replicates. *$P \leq 0.05$ indicates statistically significant differences from the control group.

by treating NCI-H460 and A549 cells with (*E*)-2,4-bis(*p*-hydroxyphenyl)-2-butenal (10–40 μg·mL^{-1}). (*E*)-2,4-bis(*p*-hydroxyphenyl)-2-butenal caused the phosphorylation of all the three MAPK proteins. The phosphorylation of ERK, cJNK and p38 was found to be increased in a concentration-dependent manner (Figure 4A). This increase in phosphorylation of MAPK proteins can be further associated with the induction of apoptosis induced by the activation of the caspase cascade.

Inhibition of the MAPK pathway reversed the effect of (E)-2,4-bis(p-hydroxyphenyl)-2-butenal

The inhibition of p38 MAPK with SB203580, but not other inhibitors (JNK and ERK), reversed the increase in apoptosis induced by (*E*)-2,4-bis(*p*-hydroxyphenyl)-2-butenal. Pretreatment with SB203580 increased the viability of both NCI-H460 and A549 cells (Figure 4B), and decreased the percentage of cells undergoing apoptosis (Figure 5A). The effect of (*E*)-2,4-bis(*p*-hydroxyphenyl)-2-butenal on the apoptotic proteins caspase-3 and -9 was also reversed by SB203580 (Figure 4C), as were its effects on NF-κB and the expression of the death receptors (Figure 4C). The colony formation assay was performed after inhibition of p38 MAPK and it was found that the number of colonies was concentration-dependently decreased by (*E*)-2,4-bis(*p*-hydroxyphenyl)-2-butenal. But the cells pretreated with p38 MAPK inhibitor had higher number of colonies compared with those treated with just (*E*)-2,4-bis(*p*-hydroxyphenyl)-2-butenal. Hence, inhibition of p38 MAPK reversed the (*E*)-2,4-bis(*p*-hydroxyphenyl)-2-butenal-induced inhibitory effect on cancer cell growth (Figure 5B). Thus, p38 MAPK plays a very important role in (*E*)-2,4-bis(*p*-hydroxyphenyl)-2-butenal-induced apoptosis.

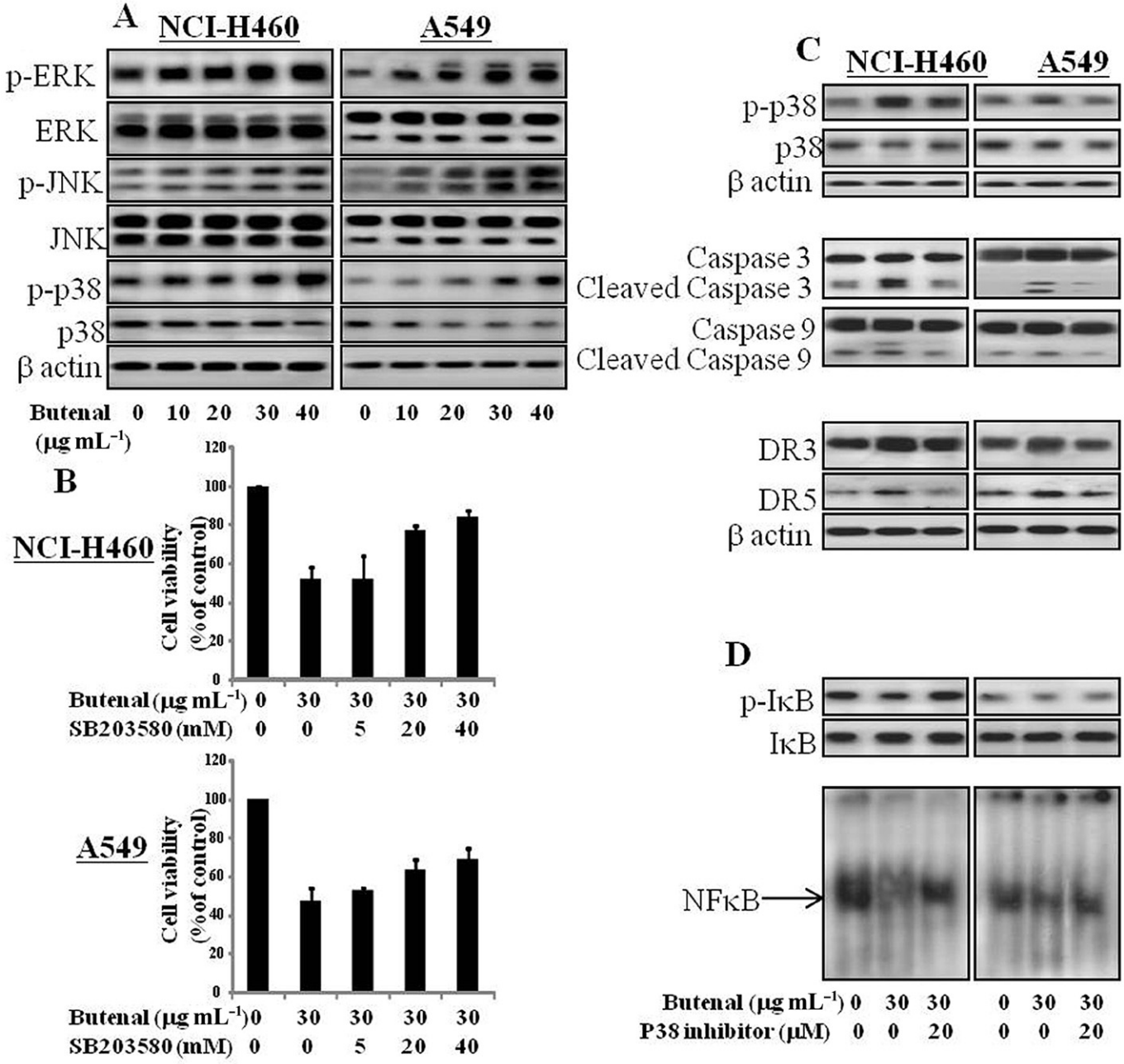

Figure 4

Effect of (*E*)-2,4-bis(*p*-hydroxyphenyl)-2-butenal on MAPK activation in NSCLC cell lines. (A) The cells were treated with different concentrations (0–40 μg·mL^{-1}) of (*E*)-2,4-bis(*p*-hydroxyphenyl)-2-butenal at 37°C of 30 min, equal amounts of total proteins (50 μg per lane) were subjected to 10% SDS-PAGE. Expressions of ERK, p-ERK, JNK, p-JNK, p38, p-p38 and β-actin were detected by Western blotting using specific antibodies. β-Actin protein was used an internal control in both NCI-H460 and A549 lung cancer cells. Each band is representative of three independent experiments. Effect of p38 inhibitor SB203580 on the activity of (*E*)-2,4-bis(*p*-hydroxyphenyl)-2-butenal. (B) The effect of pretreatment with SB203580 on the (*E*)-2,4-bis(*p*-hydroxyphenyl)-2-butenal-induced decrease in cell viability. After treatment with (*E*)-2,4-bis(*p*-hydroxyphenyl)-2-butenal (0–40 μg·mL^{-1}) for 24 h, the cells were harvested by trypsinization and stained with 0.2% trypan blue. Relative cell survival rate was determined by counting live and dead cells. (C) The effect of pretreatment with SB203580 on the (*E*)-2,4-bis(*p*-hydroxyphenyl)-2-butenal-induced increase in the death receptor expression and caspase-3 and -9 activation. (D) The effect of pretreatment with SB203580 on the (*E*)-2,4-bis(*p*-hydroxyphenyl)-2-butenal-induced NF-κB inactivation, the cells treated with (*E*)-2,4-bis(*p*-hydroxyphenyl)-2-butenal (0–40 μg·mL^{-1}) for 1 h were lysed, cytosolic proteins were used to determine the expression of IκB, p-IκB and β-actin (internal control). The effect of pretreatment with SB203580 on the (*E*)-2,4-bis(*p*-hydroxyphenyl)-2-butenal-induced inhibition of NF-κB DNA binding activity. Nuclear extracts from NCI-H460 and A549 lung cancer cells pretreated with SB203580 for 30 min and treated with (*E*)-2,4-bis(*p*-hydroxyphenyl)-2-butenal (0–40 μg·mL^{-1}) for 1 h were incubated in binding reactions of ^{32}P-end-labelled oligonucleotide containing the κB sequence. The activation of NF-κB was investigated using EMSA as described in Methods. Values are mean ± SD of three experiments with replicates. *$P \leq 0.05$ indicates statistically significant differences from the control group.

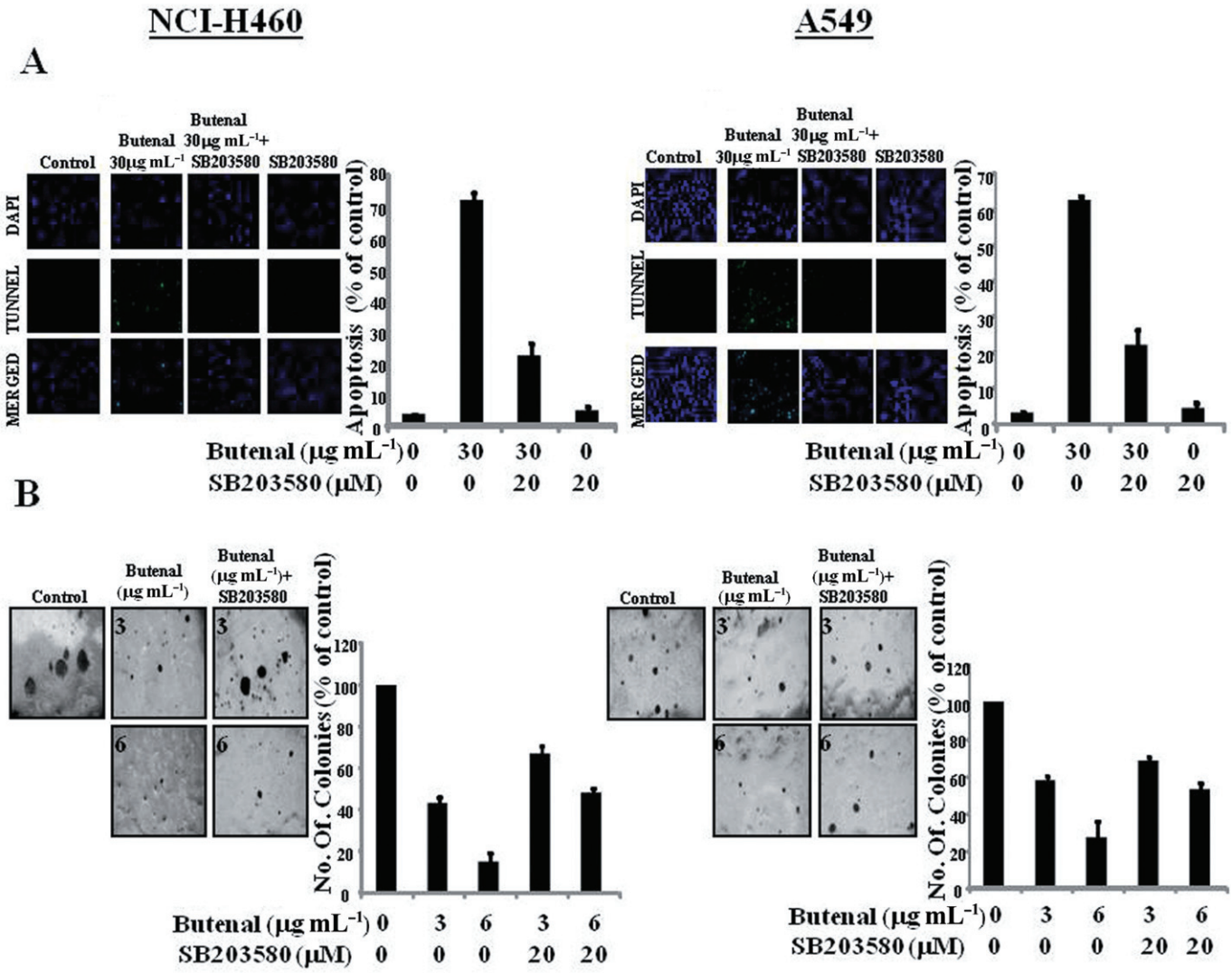

Figure 5

(A) The effect of pretreatment with SB203580 on the (*E*)-2,4-bis(*p*-hydroxyphenyl)-2-butenal-induced apoptosis, the apoptotic cell death of non-small cell lung cancer cell lines pretreated with SB203580 and then treated with (*E*)-2,4-bis(*p*-hydroxyphenyl)-2-butenal. Quantification of apoptosis by TUNEL assay. The NSCLC cells NCI-H460 and A549, were pretreated with 20 μM SB203580 for 30 min and then treated with (*E*)-2,4-bis(*p*-hydroxyphenyl)-2-butenal (30 μg·mL^{-1}) for 24 h and then labelled with TUNEL solution. The green colour in the fixed cells marks TUNEL-labelled cells. Total number of cells in a given area was determined by using DAPI nuclear staining (fluorescent microscope). The apoptotic index was determined as the DAPI-stained TUNEL-positive cell number/total DAPI-stained cell number (magnification, ×200). Values are mean ± SD of three experiments with replicates. *$P \leq 0.05$ indicates statistically significant differences from the control group. (B) The effect of pretreatment with SB203580 on the (*E*)-2,4-bis(*p*-hydroxyphenyl)-2-butenal-induced inhibition of colony formation in NCI-H460 and A549 cells. After 30 min of pretreatment 8×10^3 cell·mL^{-1} were suspended in 2 mL of 0.3% agar containing basal medium Eagle's agar containing 10% FBS. The cultures were maintained at 37°C in a 5% CO_2 atmosphere for 2 weeks, and cell colonies >80 μm in diameter were scored. Values are mean ± SD of three experiments with replicates. *$P \leq 0.05$ indicates statistically significant differences from the control group.

Knock down of TNFRSF10B reversed the effect of (E)-2,4-bis(p-hydroxyphenyl)-2-butenal

To determine the relationship between the expression of the death receptors (TNFRSF12, TNFRSF10B and TNFRSF21) and the cell growth inhibitory effect of (*E*)-2,4-bis(*p*-hydroxyphenyl)-2-butenal, we transfected NCI-H460 and A549 cells with TNFRSF12, TNFRSF10B and TNFRSF21 siRNA using a transfection agent. The viability of cells with TNFRSF10B knock down was increased significantly (Figure 6A). Hence TNFRSF10B is important for (*E*)-2,4-bis(*p*-hydroxyphenyl)-2-butenal-induced apoptosis. The cells were then transfected with 100 nM siRNA of TNFRSF10B and control for 24 h, and then treated with (*E*)-2,4-bis(*p*-hydroxyphenyl)-2-butenal. The expression of caspase-3 and 9 were found to be reversed in the TNFRSF10B transfected cells. The (*E*)-2,4-bis(*p*-hydroxyphenyl)-2-butenal-induced activation of p38 MAPK and inactivation of NF-κB was also reversed

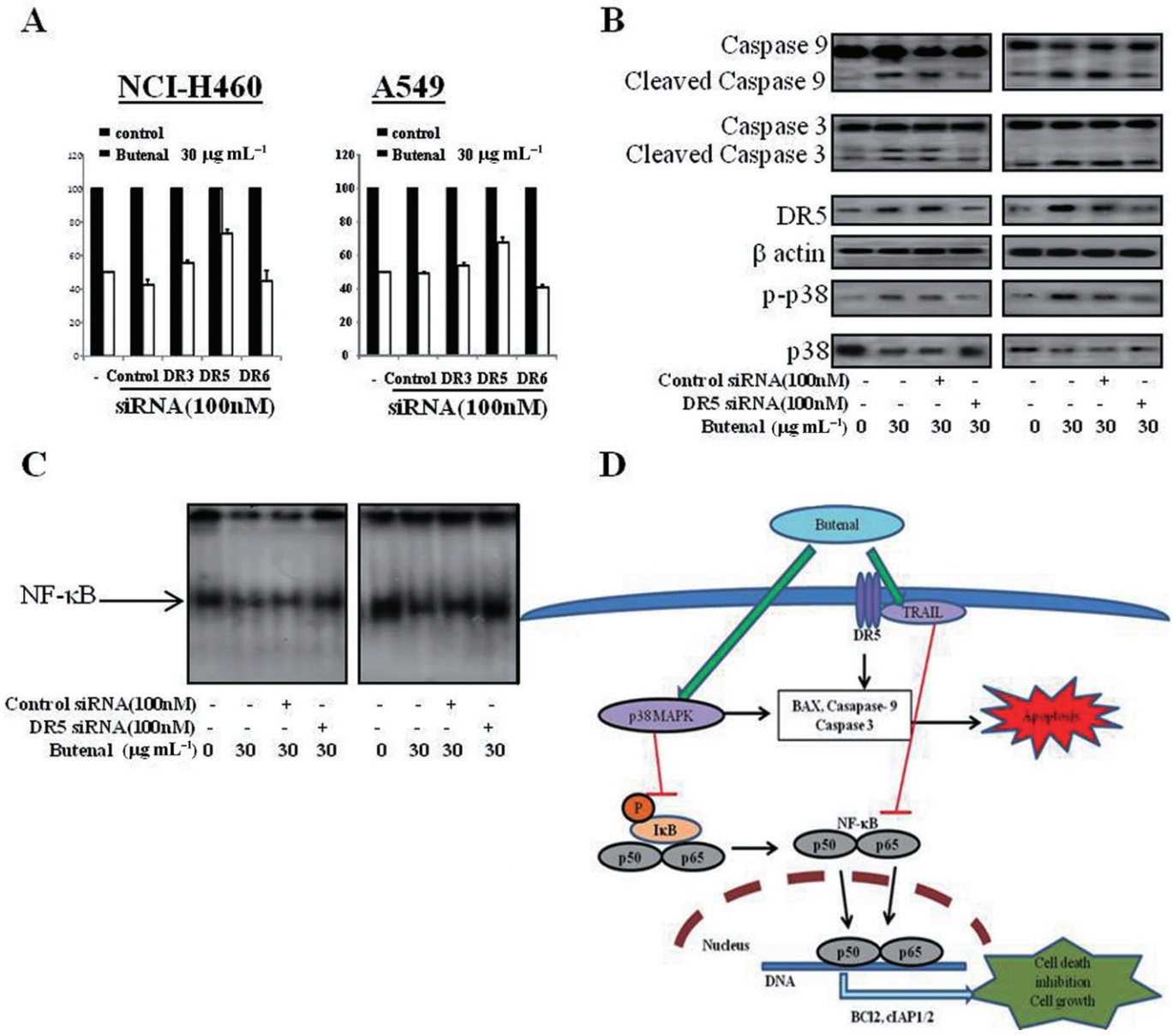

Figure 6

Effect of siRNA of TNFRSFs (death receptors) on the (*E*)-2,4-bis(*p*-hydroxyphenyl)-2-butenal-induced cancer cell growth inhibition, p38 expression and apoptosis in lung cancer cells. (A) Effect of siRNA of DR on the (*E*)-2,4-bis(*p*-hydroxyphenyl)-2-butenal-induced cell viability. The lung cancer cells were transfected with the DR siRNA (100 nM) for 24 h; the cells were then treated with (*E*)-2,4-bis(*p*-hydroxyphenyl)-2-butenal (30 μg·mL^{-1}) for another 24 h. The cells were harvested by trypsinization and stained with 0.2% trypan blue. Relative cell survival rate was determined by counting live and dead cells. Values are mean ± SD of three experiments with replicates. $^{*}P \leq 0.05$, significantly different from untreated control cells. $^{\#}P \leq 0.01$, significantly different from control siRNA transfected cells. (B) The cells were transfected with non-targeting control siRNA or TNFRSF10B (DR5) siRNA (100 nM) as described in Methods for 24 h. Then (*E*)-2,4-bis(*p*-hydroxyphenyl)-2-butenal was treated (30 μg·mL^{-1}) at 37°C. Equal amounts of total proteins (50 μg·per lane) were subjected to 10% SDS-PAGE. Expressions of cleaved caspase-3, cleaved caspase-9, TNFRSF10B, p38, p-p38 and β-actin were detected by Western blotting using specific antibodies. β-Actin protein was used an internal control in NCI-H460 and A549 lung cancer cells. Each band is representative of three independent experiments. (C) Effect of siRNA of TNFRSF10B (DR5) on the (*E*)-2,4-bis(*p*-hydroxyphenyl)-2-butenal-induced NF-κB inactivation. Nuclear extract from NCI-H460 and A549 lung cancer cells pre-treated with SB203580 of 30 min and treated with (*E*)-2,4-bis(*p*-hydroxyphenyl)-2-butenal (0–40 μg·mL^{-1}) for 1 h was incubated in binding reactions of ^{32}P-end-labelled oligonucleotide containing the κB sequence. The activation of NF-κB was investigated using EMSA as described in Methods. Values are mean ± SD of three experiments with replicates. $^{*}P \leq 0.05$ indicates statistically significant differences from the control group. (D) Schematic representation of anti-proliferative effect of (*E*)-2,4-bis(*p*-hydroxyphenyl)-2-butenal on NSCLC cells.

in TNFRSF10B knock down cells (Figure 6B). These results indicate that the TNFRSF10B pathway is significantly involved in (*E*)-2,4-bis(p-hydroxyphenyl)-2-butenal-induced lung cancer cell death.

Discussion

The central point of interest in the present study is the nature of the inhibitory effect of (*E*)-2,4-bis(*p*-hydroxyphenyl)-2-butenal on the growth of NSCLC cells (NCI-H460 and A549). This inhibitory effect was shown to be due to apoptosis, which was found to be induced by the stimulation of TNFRSF10B that then mediated the activation of caspase-3 and caspase-9. (*E*)-2,4-bis(*p*-hydroxyphenyl)-2-butenal was also found to inactivate NF-κB, a major transcriptional factor in cellular events. Activation of p38 MAPK was also associated with the increased apoptotic cell death induced by (*E*)-2,4-bis(*p*-hydroxyphenyl)-2-butenal. However inhibition of p38 MAPK and knock down of TNFRSF10B reversed the (*E*)-2,4-bis(*p*-hydroxyphenyl)-2-butenal-induced inhibitory effect on cancer cell growth and colony formation, caspase-3 and -9 activation as well as NF-κB inactivation. Thus, (*E*)-2,4-bis(*p*-hydroxyphenyl)-2-butenal has an anti-proliferative effect induced by p38 MAPK-mediated TNFRSF10B-dependent caspase-3 and -9 activation and NF-κB inactivation.

(*E*)-2,4-bis(*p*-hydroxyphenyl)-2-butenal induces antioxidant and anti-inflammatory effects through inhibition of NF-κB and STAT3 activity in LPS-stimulated astrocytes and microglial BV-2 cells (Lee *et al.*, 2011a). Furthermore, (*E*)-2,4-bis(*p*-hydroxyphenyl)-2-butenal also significantly inhibits colon tumour growth *in vivo* (xenograft assay). In a study on colon cancer cells, we found that (*E*)-2,4-bis(*p*-hydroxyphenyl)-2-butenal affected NF-κB activity (evidenced by docking model and pull down assay), and at a similar range of concentrations, it also inhibited colon cancer cell growth too (unpublished observations).

Activated death receptors induce apoptosis through the activation of downstream caspases, including caspases-9 and -3, as well as the translocation of Bax to mitochondria (Elrod and Sun, 2008). Various compounds, such as Chan Su (*Venenum Bufonis*) and indole-3-carbinol, have been shown to induce apoptosis by death receptor-mediated caspase-3 and -9 activation in NSCLC cell lines (Yun *et al.*, 2009; Choi *et al.*, 2010). Activation of caspase-3 and -9 also induces apoptosis in lung cancer cells. Diallyl trisulfide was found to induce apoptosis of A549 lung cancer cells by activation of caspase-3 and -9 both *in vitro* and *in vivo* (Li *et al.*, 2012). Further, luteolin was shown to induce apoptosis of lung cancer cells via caspase-3 and caspase-9 activation (Chen *et al.*, 2012). Among the death receptors, the TNF-related apoptosis-inducing ligand receptors TNFRSF10A (TRAIL-R1) and TNFRSF10B (TRAIL-R2) are selectively expressed in cancer cells and thus offer an advantage for targeted therapy and prevention (Srivastava, 2000; Srivastava, 2001; Shankar and Srivastava, 2004). Aclarubicin enhances TRAIL-induced apoptosis through TNFRSF10B up-regulation in A549 NSCLC cells via the expression of caspase-3, -8 and -9 (Horinaka *et al.*, 2012). 5-Allyl-7-gen-difluoromethoxychrysin synergistically enhances TRAIL-mediated apoptosis in NSCLC cells by up-regulating TNFRSF10B and increasing the expression of caspase-3 and caspase-9 (Xie *et al.*, 2011). Sorafenib induces apoptotic cell death in human NSCLC cells (A549 and NCI-H460) by sensitizing the cells to TRAIL-induced up-regulation of TNFRSF10B (Kim *et al.*, 2011). Thus, the increased expression of cleaved caspase-3 and -9 were correlated with the increased expression of TRAIL and TNFRSF10B. Similarly, our data demonstrated that (*E*)-2,4-bis(*p*-hydroxyphenyl)-2-butenal increased expression of TRAIL and TNFRSF10B, but there is no change in the expression of TNFRSF10A. This increase in TNFRSF10B was associated with caspase-3 and -9 activation and Bax expression. Even though TNFRSF12 and TNFRSF21 were increased by the treatment with (*E*)-2,4-bis(*p*-hydroxyphenyl)-2-butenal, TNFRSF12 and TNFRSF21 knockdown did not change the inhibitory effect of (*E*)-2,4-bis(*p*-hydroxyphenyl)-2-butenal on lung cancer cell growth. However, the knock down of TNFRSF10B with small interfering RNA (siRNA) reversed the inhibitory effect of (*E*)-2,4-bis(*p*-hydroxyphenyl)-2-butenal on cell growth and the expression of cleaved caspase-3 and -9. Thus, activation of the TNFRSF10B pathway could be important for the (*E*)-2,4-bis(*p*-hydroxyphenyl)-2-butenal-induced apoptotic death of NSCLC cells.

The signalling event implicated in survival, growth arrest or programmed cell death includes activation of the MAPK pathway (Schwenger *et al.*, 1998). The p38 MAPK was found to be significantly involved in the chemotherapy-induced death of many cancer cells (Chang and Karin, 2001). Metformin treatment of lung cancer cells activates the JNK/p38 MAPK signalling pathway and caspase-3. Blockade of the JNK/p38 MAPK pathway prevented the apoptosis induced by metformin (Wu *et al.*, 2011). Curcumin rapidly induces activation of the MAPK including ERK1/2 and JNK to induce cell death in tumour cells. Inhibition of JNK (with SP600125) or ERK1/2 (with U0126) partially prevented curcumin-induced cell death in various cancer cells including human rhabdomyosarcoma cells (Rh30), Ewing sarcoma (Rh1), colon adenocarcinoma (HT29) and cervical cancer (HeLa) cells (Han *et al.*, 2012). Crotoxin (CrTX) has anti-tumour effects on A549 lung cancer cells, inducing apoptosis by activation of p38 MAPK and caspase-3 (Ye, 2011). Benzyl isothiocyanate (BITC) and phenethyl isothiocyanate (PEITC) suppress the metastasis potential of highly metastatic lung cancer cells by inducing apoptosis through the targeting of the p38 and JNK MAPK pathway (Yan *et al.*, 2011). 4-Phenyl-3-butenoic acid (PBA), an experimental compound, reverses the transformed phenotype at non-cytotoxic concentrations and activates p38 MAPK in human lung carcinoma and Ras-transformed cells, effects that correlate well with decreased cell growth and increased cell–cell communication (Matesic *et al.*, 2012). MAPK pathways are activated in A549 cells infected with Newcastle disease, and p38 MAPK has been found to be involved in Newcastle disease virus-induced cell death, induced by activation of caspase-3 and –9 (Bian *et al.*, 2011). An isoquinoline, AM6-36, induces apoptosis of HL-60 human leukaemia cells by activation of MAPKs (p38 and JNK) (Park *et al.*, 2012). Taken together, p38 MAPK activation can induce apoptosis of various cancer cells, including lung cancer cells, by increasing the expression of cleaved caspase-3 and -9. Moreover, previous reports have indicated that p38 is the upstream target of TNFRSF10B induced by other agents (Lei *et al.*, 2008; Park *et al.*, 2010). Phenethyl isothiocyanate

stimulated TNFRSF10B to induce apoptosis in human oral cancer cells via p38 MAPK (Huong *et al.*, 2012). It was also found that AW00179 has the potential to sensitize H1299 NSCLC cells to TRAIL-mediated apoptosis through two distinct mechanisms: ROS-JNK-c-Jun-(MAPK)-mediated up-regulation of TNFRSF10B and the down-regulation of anti-apoptotic molecules (Hwang *et al.*, 2012b). Nimbolide sensitizes human colon cancer cells as well as H1299 lung cancer cells to TRAIL through ROS- and ERK-dependent up-regulation of TNFRSF10A and B, cleaved caspase-3 and -9, p53 and Bax (Gupta *et al.*, 2011). Hence, the activation of p38 MAPK leads to an increased expression of TNFRSF10B, and consequently an increased expression of cleaved caspase-3 and -9 and apoptosis (Huong *et al.*, 2012). Similar to these findings, our data showed that the p38 MAPK pathway is concomitantly activated during (*E*)-2,4-bis(*p*-hydroxyphenyl)-2-butenal-induced lung cancer cell death. We further found that inhibition of p38 MAPK reversed the inhibitory effect of (*E*)-2,4-bis(*p*-hydroxyphenyl)-2-butenal on cell growth, its ability to increase the expressions of TNFRSF10B, caspase-3 and -9. Thus, activation of the p38 MAPK pathway may have an important role in (*E*)-2,4-bis(*p*-hydroxyphenyl)-2-butenal-induced apoptosis of NSCLC cells mediated through activation of the TNFRSF10B pathway.

Members of the NF-κB family also play an important role in the development and progression of several human malignancies (Baud and Karin, 2009; Nakshatri *et al.*, 1997). It is known that NF-κB exerts its anti-apoptotic activity through induction of many anti-apoptotic factors including c-IAP1, and 2, XIAP, Bcl-2 and Bcl-x L. These anti-apoptotic factors inhibit apoptosis induced by the death receptor-mediated pathways by directly binding to and inhibiting death inducers (Roya *et al.*, 2008). Thus activation of NF-κB is correlated with resistance to apoptosis and anti-apoptotic properties. Recent studies on the signalling mechanisms of the death receptor revealed that members of the NF-κB and caspase families are key regulators of cell death. Moreover, it was found that genes like TNFAIP3 and NFκBIA, which are up-regulated by TRAIL, are inhibitors of the NF-κB pathway (Cooper *et al.*, 1996; Daigeler *et al.*, 2008). The combination of TRAIL and taurolidine caused apoptosis in human fibrosarcoma cells by inactivation of NF-κB (Daigeler *et al.*, 2008). A novel parthenin analogue exhibits anticancer activity by inactivation of NF-κB and up-regulation of TNFRSF10B in human leukaemia HL-60 cells (Kumar *et al.*, 2011). Thus, it is possible that the inactivation of NF-κB correlates with the increased expression of TNFRSF10B. 2-Hydroxycinnamaldehyde is involved in MAPK (ERK)-dependent inactivation of NF-κB in TNF-α-treated SW620 colon cancer cells and induces apoptosis by caspase-3 and -9 (Lee *et al.*, 2005). The xenobiotic-induced oxidative stress leads to activation of the MAPK pathway ERK, JNK or p38, and blocking of the NF-κB pathway, which results in increased expression of the death receptor gene and activation of the ICE/Ced-3 (caspase) pathway leading to cell death and an apoptotic response (Kong *et al.*, 2000). We found that knock down of TNFRSF10B with a siRNA reversed the (*E*)-2,4-bis(*p*-hydroxyphenyl)-2-butenal-induced activation of p38 MAPK and inactivation of NF-κB. Similarly the inhibition of p38 MAPK reversed (*E*)-2,4-bis(*p*-hydroxyphenyl)-2-butenal-induced activation of TNFRSF10B and inactivation of NF-κB. Thus, inhibition of NF-κB-mediated activation of MAPK and the death receptor may cause apoptosis in cancer cells. Hence, inactivation of NF-κB was associated with an increase in the expression of TNFRSF10B and MAPK. Thus, inactivation of NF-κB also augments the (*E*)-2,4-bis(*p*-hydroxyphenyl)-2-butenal-induced apoptosis signaling pathway.

We conclude that (*E*)-2,4-bis(*p*-hydroxyphenyl)-2-butenal induces apoptosis in NSCLC cells by p38 MAPK- mediated inactivation of NF-κB and activation of TNFRSF10B, which then activates the caspase-3 and caspase-9 pathways.

Acknowledgements

This work was supported by the National Research Foundation of Korea (NRF) grant funded by the Korea government [MEST] (MRC, 2011–0028213).

Conflicts of interest

None.

References

Ashkenazi A (2002). Targeting death and decoy receptors of the tumor-necrosis factor super family. Nat Rev Cancer 2: 420–430.

Atrooz OM (2008). The effects of Maillard reaction products on apple and potato polyphenoloxidase and their antioxidant activity. Int J Food Sci Technol 43: 490–494.

Baud V, Karin M (2001). Signal transduction by tumor necrosis factor and its relatives. Trends Cell Biol 11: 372–377.

Baud V, Karin M (2009). Is NF-kappaB a good target for cancer therapy? Hopes and pitfalls. Nat Rev Drug Discov 8: 33–40.

Bian J, Wang K, Kong X, Liu H, Chen F, Hu M *et al.* (2011). Caspase- and p38-MAPK-dependent induction of apoptosis in A549 lung cancer cells by Newcastle disease virus. Arch Virol 156: 1335–1344.

Chang L, Karin M (2001). Mammalian MAP kinase signalling cascades. Nature 410: 37–40.

Chen Q, Liu S, Chen J, Zhang Q, Lin S, Chen Z *et al.* (2012). Luteolin induces mitochondria-dependent apoptosis in human lung adenocarcinoma cell. Nat Prod Commun 7: 29–32.

Choi HS, Cho MC, Lee HG, Yoon DY (2010). Indole-3-carbinol induces apoptosis through p53 and activation of caspase-8 pathway in lung cancer A549 cells. Food Chem Toxicol 48: 883–890.

Cooper JT, Stroka DM, Brostjan C, Palmetshofer A, Bach FH, Ferran C (1996). A20 blocks endothelial cell activation through a NF-kappaB-dependent mechanism. J Biol Chem 271: 18068–18073.

Daigeler A, Brenzel C, Bulut D, Geisler A, Hilgert C, Lehnhardt M *et al.* (2008). TRAIL and Taurolidine induce apoptosis and decrease proliferation in human fibrosarcoma. J Exp Clin Cancer Res 27: 82.

Elrod HA, Sun SY (2008). Modulation of death receptors by cancer therapeutic agents. Cancer Biol Ther 7: 163–173.

Gupta SC, Reuter S, Phromnoi K, Park B, Hema PS, Nair M *et al.* (2011). Nimbolide sensitizes human colon cancer cells to TRAIL through reactive oxygen species- and ERK-dependent up-regulation of death receptors, p53, and Bax. J Biol Chem 286: 1134–1146.

Han X, Xu B, Beevers CS, Odaka Y, Chen L, Liu L *et al.* (2012). Curcumin inhibits protein phosphatases 2A and 5, leading to activation of mitogen-activated protein kinases and death in tumor cells. Carcinogenesis 33: 868–875.

Horinaka M, Yoshida T, Nakata S, Shiraishi T, Tomosugi M, Yoshikawa S *et al.* (2012). Aclarubicin enhances tumor necrosis factor-related apoptosis-inducing ligand-induced apoptosis through death receptor 5 upregulation. Cancer Sci 103: 282–287.

Huong L, Shin JA, Choi ES, Cho NP, Kim H, Leem DH *et al.* (2012). β-Phenethyl isothiocyanate induces death receptor 5 to induce apoptosis in human oral cancer cells via p38. Oral Dis 18: 513–519.

Hwang IG, Hyun YK, Sang HL, Koan SW, Jung OB, Jin TH *et al.* (2012a). Isolation and identification of an antiproliferative substance from fructose–tyrosine Maillard reaction products. Food Chem 130: 547–551.

Hwang MK, Ryu BJ, Kim SH (2012b). AW00179 potentiates TRAIL-mediated death of human lung cancer H1299 cells through ROS-JNK-c-Jun-mediated up-regulation of DR5 and down-regulation of anti-apoptotic molecules. Amino Acids 43: 1679–1687.

Jing H, Kitts DD (2004). Antioxidant activity of sugar-lysine Maillard reaction products in cell free and cell culture systems. Arch Biochem Biophys 429: 154–163.

Karin M, Greten FR (2005). NF-kappaB: linking inflammation and immunity to cancer development and progression. Nat Rev Immunol 5: 749–759.

Karin M, Lin A (2002). NF-kappaB at the crossroads of life and death. Nat Immunol 3: 221–227.

Kim YH, Lee SH, Lee JY, Choi SW, Park JW, Kwon TK (2004). Triptolide inhibits murine-inducible nitric oxide synthase expression by down-regulating lipopolysaccharide-induced activity of nuclear factor-kappa B and c-Jun NH2-terminal kinase. Eur J Pharmacol 494: 1–9.

Kim YS, Jin HO, Seo SK, Woo SH, Choe TB, An S *et al.* (2011). Sorafenib induces apoptotic cell death in human non-small cell lung cancer cells by down regulating mammalian target of rapamycin (mTOR)-dependent survivin expression. Biochem Pharmacol 82: 216–226.

Kong AN, Yu R, Chen C, Mandlekar S, Primiano T (2000). Signal transduction events elicited by natural products: role of MAPK and caspase pathways in homeostatic response and induction of apoptosis. Arch Pharm Res 23: 1–16.

Kumar A, Malik F, Bhushan S, Shah BA, Taneja SC, Pal HC *et al.* (2011). A novel parthenin analog exhibits anti-cancer activity: activation of apoptotic signaling events through robust NO formation in human leukemia HL-60 cells. Chem Biol Interact 193: 204–215.

Lee FS, Hagler J, Chen ZJ, Maniatis T (1997). Activation of the IkappaB alpha kinase complex by MEKK1, a kinase of the JNK pathway. Cell 88: 213–222.

Lee SH, Lee CW, Lee JW, Choi MS, Son DJ, Chung YB *et al.* (2005). Induction of apoptotic cell death by 2′-hydroxycinnamaldehyde is involved with ERK-dependent inactivation of NF-kappaB in TNF-alpha-treated SW620 colon cancer cells. Biochem Pharmacol 70: 1147–1157.

Lee YJ, Choi DY, Choi IS, Han JY, Jeong HS, Han SB *et al.* (2011a). Inhibitory effect of a tyrosine-fructose Maillard reaction product, 2,4-bis(p-hydroxyphenyl)-2-butenal on amyloid-β generation and inflammatory reactions via inhibition of NF-κB and STAT3 activation in cultured astrocytes and microglial BV-2 cells. J Neuroinflammation 8: 132.

Lee YJ, Lee YM, Lee CK, Jung JK, Han SB, Hong JT (2011b). Therapeutic applications of compounds in the Magnolia family. Pharmacol Ther 130: 157–176.

Lei P, Abdelrahim M, Cho SD, Liu X, Safe S (2008). Structure-dependent activation of endoplasmic reticulum stress-mediated apoptosis in pancreatic cancer by 1,1-bis(3′-indoly) 1-(p-substituted phenyl)methanes. Mol Cancer Ther 7: 3654.

Li W, Tian H, Li L, Li S, Yue W, Chen Z *et al.* (2012). Diallyl trisulfide induces apoptosis and inhibits proliferation of A549 cells in vitro and in vivo. Acta Biochim Biophys Sin (Shanghai) 44: 577–583.

Locksley RM, Killeen N, Lenardo MJ (2001). The TNF and TNF receptor superfamilies: integrating mammalian biology. Cell 104: 487–501.

Matesic DF, Sidorova TS, Burns TJ, Bell AM, Tran PL, Ruch RJ *et al.* (2012). p38 MAPK activation, JNK inhibition, neoplastic growth inhibition, and increased gap junction communication in human lung carcinoma and Ras-transformed cells by 4-phenyl-3-butenoic acid. J Cell Biochem 113: 269–281.

Moon DO, Park SY, Lee KJ, Heo MS, Kim KC, Kim MO *et al.* (2007). Bee venom and melittin reduce proinflammatory mediators in lipopolysaccharide-stimulated BV2 microglia. Int Immunopharmacol 7: 1092–1101.

Nakshatri H, Bhat-Nakshatri P, Martin DA, Goulet RJ Jr, Sledge GW Jr (1997). Constitutive activation of NF-kappaB during progression of breast cancer to hormone-independent growth. Mol Cell Biol 17: 3629–3639.

Nesbitt JC, Lee JS, Komaki R, Roth JA (1997). Cancer of the lung. In: Holland JF, Bast RC, Morton DL, Frei E, Kufe DW, Weichselbaum RR (eds). Cancer Medicine, Williams and Wilkins: Baltimore, pp. 1723–1795.

Park EJ, Kiselev E, Conda-Sheridan M, Cushman M, Pezzuto JM (2012). Induction of apoptosis by 3-amino-6- (3-aminopropyl) -5,6-dihydro-5,11-dioxo-11H-indeno [1,2-c] isoquinoline via modulation of MAPKs (p38 and c-Jun N-terminal kinase) and c-Myc in HL-60 human leukemia cells. J Nat Prod 75: 378–384.

Park SK, Sanders BG, Kline K (2010). Tocotrienols induce apoptosis in breast cancer cell lines via an endoplasmic reticulum stress-dependent increase in extrinsic death receptor signaling. Breast Cancer Res Treat 124: 361–375.

Rigas JR (1998). Do newer chemotherapeutic agents improve survival in non-small cell lung cancer? Semin Oncol 25: 5–9.

Roya K-F, Zahra Z, Richard A (2008). Lockshin, Programmed Cell Death, the Biology and Therapeutic Implications of Cell Death. 446: 450.

Schwenger P, Alpert D, Skolnik EY, Vilcek J (1998). Activation of p38 mitogen-activated protein kinase by sodium salicylate leads to inhibition of tumor necrosis factor-induced IkappaB alpha phosphorylation and degradation. Mol Cell Biol 18: 78–84.

Shankar S, Srivastava RK (2004). Enhancement of therapeutic potential of TRAIL by cancer chemotherapy and irradiation: mechanisms and clinical implications. Drug Resist Updat 7: 139–156.

Srivastava RK (2000). Intracellular mechanisms of TRAIL and its role in cancer therapy. Mol Cell Biol Res Commun 4: 67–75.

Srivastava RK (2001). TRAIL/Apo-2L: mechanisms and clinical applications in cancer. Neoplasia 3: 535–546.

Viatour P, Merville MP, Bours V, Chariot A (2005). Phosphorylation of NF-kappaB and IkappaB proteins: implications in cancer and inflammation. Trends Biochem Sci 30: 43–52.

Wang X, Martindale JL, Holbrook NJ (2000). Requirement for ERK activation in cisplatin-induced apoptosis. J Biol Chem 275: 39435–39443.

Wu N, Gu C, Gu H, Hu H, Han Y, Li Q (2011). Metformin induces apoptosis of lung cancer cells through activating JNK/p38 MAPK pathway and GADD153. Neoplasma 58: 482–490.

Xie ZH, Quan MF, Liu F, Cao JG, Zhang JS (2011). 5-allyl-7-gen-difluoromethoxychrysin enhances TRAIL-induced apoptosis in human lung carcinoma A549 cells. BMC Cancer 11: 322.

Yan H, Zhu Y, Liu B, Wu H, Li Y, Wu X *et al*. (2011). Mitogen-activated protein kinase mediates the apoptosis of highly metastatic human non-small cell lung cancer cells induced by isothiocyanates. Br J Nutr 106: 1779–1791.

Ye B, Xie Y, Qin ZH, Wu JC, Han R, He JK (2011). Anti-tumor activity of CrTX in human lung adenocarcinoma cell line A549. Acta Pharmacol Sin 32: 1397–1401.

Yun HR, Yoo HS, Shin DY, Hong SH, Kim JH, Cho CK *et al*. (2009). Apoptosis induction of human lung carcinoma cells by Chan Su (Venenum Bufonis) through activation of caspases. J Acupunct Meridian Stud 2: 210–217.

Supporting information

Additional Supporting Information may be found in the online version of this article at the publisher's web-site:

Figure S1 (A) Effect of (*E*)-2, 4-bis(*p*-hydroxyphenyl)-2-butenal (0–40 μg mL^{-1}) on the expression of COX-2, cyclin D1, MMP-9 and VEGF. Equal amounts of total proteins (50 μg·per lane) were subjected to 10% SDS-PAGE. β-Actin protein was used an internal control in NCI-H460 and A549 lung cancer cells. Each band is representative of three independent experiments. (B) Effect of vehicle on cell growth system; 0.01% and 0.02% of DMSO is treated in NCI-H460 and A549 lung cancer cells and the viability of cells is compared to control as percent.